

We are IntechOpen, the world's leading publisher of Open Access books Built by scientists, for scientists

6,900

Open access books available

186,000

International authors and editors

200M

Downloads

Our authors are among the

154

Countries delivered to

TOP 1%

most cited scientists

12.2%

Contributors from top 500 universities



WEB OF SCIENCE™

Selection of our books indexed in the Book Citation Index
in Web of Science™ Core Collection (BKCI)

Interested in publishing with us?
Contact book.department@intechopen.com

Numbers displayed above are based on latest data collected.
For more information visit www.intechopen.com



Natural Radioactive Decay

Entesar H. Elaraby

Abstract

This chapter is primarily concerned with natural radioactive decay. Generally speaking, there are two types of natural radioactive decays: alpha decays “which contain two neutrons and two protons” emitted from radon gas; additionally, nuclear decay by emission of photons (γ -decay). This chapter aims to describe γ and alpha loss of nuclei and demonstrates how to measure the radioactive material naturally using solid-state nuclear track detector (SSNTD) and high purity Germanium detector (HPGD). Also, methods of measuring the different characteristics of the alpha particle using the track profile technique (TPT) will be presented. Finally, results will be presented in the alpha and radon measurements. The concentration of aerosols has attracted much attention by many researchers in the past decade. Research has shown that aerosols are responsible for harmful chemical reactions that lead to the physical degradation of the stratospheric ozone layer. Moreover, aerosols increase the risk of developing cancer in humans when inhaled in large proportions. Therefore, neutron activation analysis (NAA) is a very important application to measure these concentrations.

Keywords: alpha particle, radon, HPGD, SSNTD, NAA, TPT

1. The source of natural radioactive

There are multiple sources that cause natural radiation. These sources are limited to three main types: cosmic radiation, internal or ground radiation.

1.1 Cosmic radiation

The Earth is constantly bombarded by cosmic rays that affect all living things. The charged particles in the radiation interact with the Earth’s magnetic field and result in an overflow of radiation from beta and gamma, the intensity of which and the value of the radiation dose differ according to the different nature of the place and the effect of the magnetic field in it [1].

1.2 Internal or ground radiation

Ground or internal radiation is present in everything that surrounds us, such as water, air and vegetation. Different levels of radioactive material from uranium, its daughters, thorium and its daughters, have been found in various places on Earth. The radiation levels vary depending on where they are measured and depend on the amount of uranium and thorium atoms present in the soil. Exposure to radiation occurs by inhaling radon gas, one of the sons of uranium and thorium, or ingesting radioactive atoms in food and water, where there are proportions of them that vary

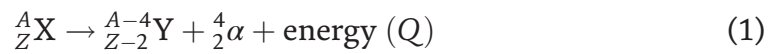
according to the location. Sites with high levels of radiation have higher dose levels [2]. High doses cause lung cancer and pose a major threat to human health [3]. Therefore it is important to measure the ground radiation from uranium and uranium decay, such as thorium, radium, and radon.

2. Radioactive decay

2.1 Alpha decay

The process of unstable (or radioactive) atoms becomes stable by emitting radiation. This event over time is called radioactive decay.

Alpha decay results in the loss of two protons and two neutrons from the nucleus.



X is parent atom and Y is daughter atom, and Q the energy is carried away primarily by the kinetic energy of the alpha particle.

Alpha particles are often observed to be produced on their own energy, meaning that the parent nucleus is converted to the basic state of the daughter's nucleus by emitting a particle with energy that corresponds to the value of the entire Q. But the degradation processes of the alpha particles may be associated with the emission of photons. As shown in **Figure 1**. This indicates the presence of energy levels and the underlying quantum structure of separate states in the nuclei as in atomic transformations. The nucleus decomposes into the excited state of the daughter's nucleus, in which case the lowest effective Q_α value. The daughter nucleus can later decay to ground state by releasing a photon. Hence a series of decay occurs

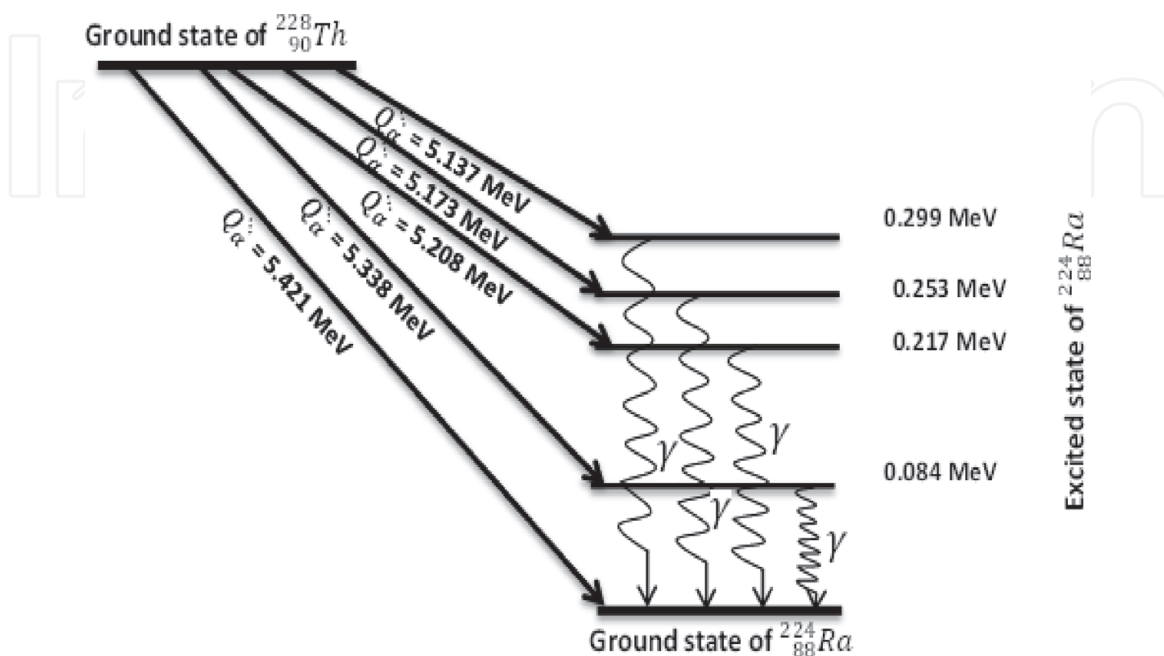
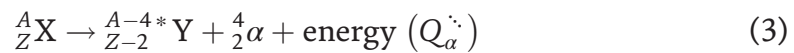


Figure 1. Alpha particle transitions in the decay of ${}^{228}\text{Th}$. Source: Das and Ferbel.

2.2 Gamma decay

A gamma ray γ has very high electromagnetic radiation carrying energy away from the nucleus.



When a nucleus disintegrates by emitting an α -particle or a β -particle, the daughter nucleus may be left in an excited state, if the excited nucleus does not break apart or emit another particle, it can de-excite to the ground state by emitting a high energy photon or gamma (γ) ray. As we see in **Figure 2**.



3. Measurement of radioactive

3.1 Measurement of alpha particle and radon

The Solid State Nuclear Track Detector SSNTDs is a polymer used for detecting energetic charged particles such as protons and alpha-particles. SSNTDs are naturally occurring and manmade insulating solids and there are many types of this detector such as: inorganic crystals, glasses and plastics.

The CR-39 Solid State Nuclear Track Detector is known to be widely used for radon gas measurement. CR39 is sensitive also to detect proton and neutron dosimeter and cosmic ray investigations. The ability of CR-39 to record the location of a radiation source, even at extremely low concentrations is exploited in autoradiography studies with alpha particles, and for detection of alpha emitters. The interaction of the energetic particles with the polymer results in the formation of latent tracks. These latent tracks can be made by chemical etching of the polymer.

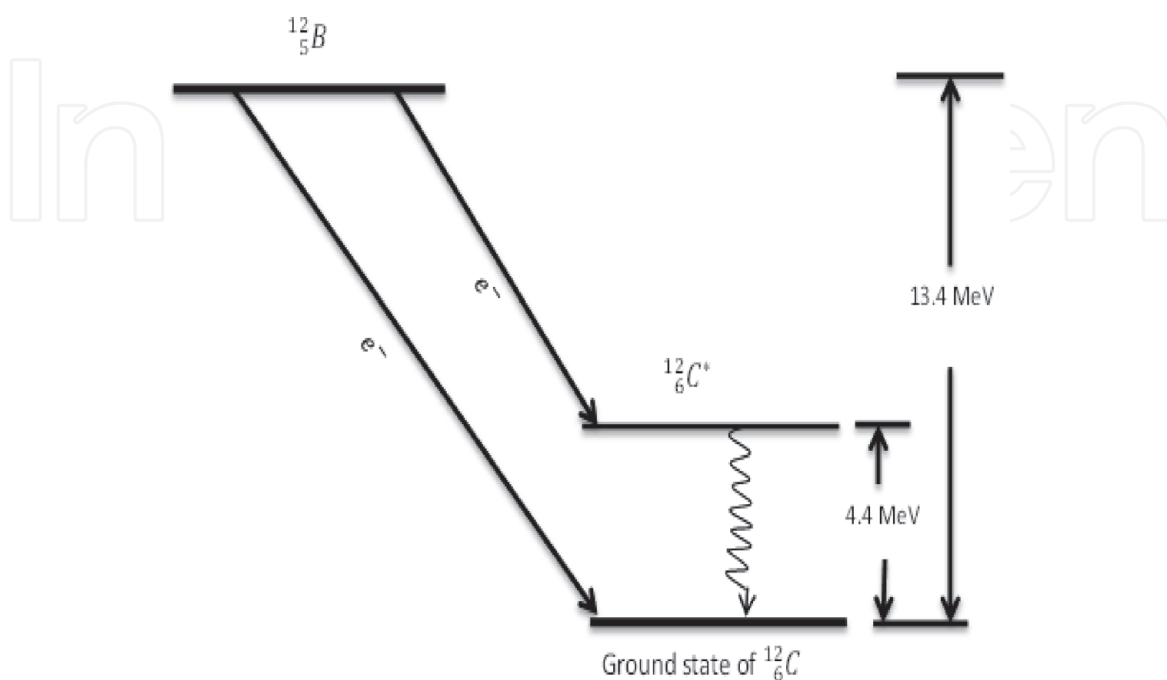


Figure 2.
 Gamma ray emitting from transitions in the decay of ${}^{12}\text{B}$.

CR-39 sheets is cut into small detectors of area $1.2 \text{ cm} \times 1.5 \text{ cm}$ each. The exposure time for sample is 30 days (to reach secular equilibrium) for ^{222}Rn determination see **Figure 3**.

After exposure the CR-39 detectors were etched in 6.25 normal NaOH at 70°C for 6 h. The different parameter of track such as the track density ρ , track diameter D and track length L are measured by using optical microscope. **Figure 4** shows that the track of particle which incidence on the surface of detector [4, 5].

To measure the Track Profile Technique (TPT) of alpha particle as **Figure 5** you must irradiate the sides (the edges) of the detector by ^{241}Am source of alpha particle with energy of five under normal incidence.

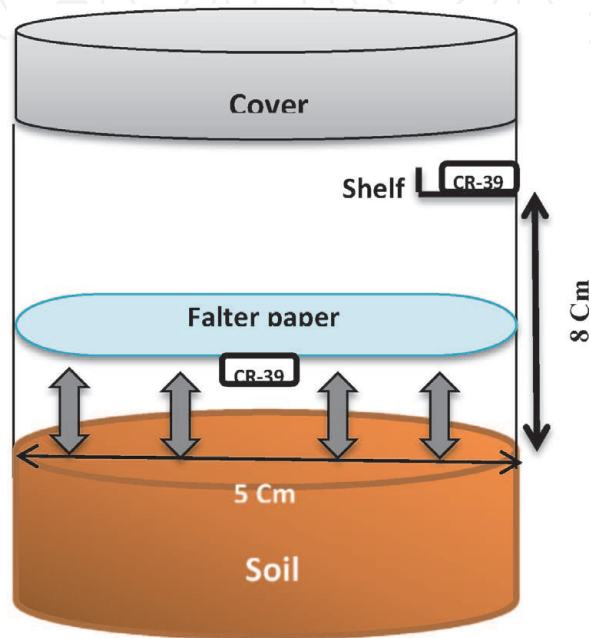


Figure 3.
The chamber used to measure the radon and alpha in soil.



Figure 4.
The reading under the microscope.

h μm	The energy of alpha 5 MeV		
	Le μm	Track profile	The type of region
5.12	6.20		The conical region $V_T > V_B$
7.68	10.00		
12.48	17.40		
14.08	17.20		The over etched region $V_T < V_B$
16.64	17.20		

Figure 5.
 The track profile of deferent energy of alpha particle at deferent bulk etch rate.

3.2 Determination of the bulk etching rate V_B and range of alpha particle

The method involves a direct measurement of the track lengths in both phases of evolution; the acute-conical and the over etched phases. Accordingly, the maximum value of the track length (L_{max}) at the saturation point and also the corresponding saturation time (t_{sat}), which is the time required for track length to reach the maximum and constant value, to be determined in accordance with the energy of the alpha particle which in turn can be used to calculate V_B according to the relation [6].

$$V_B = \frac{R_{\text{th}} - L_{\text{max}}}{t_{\text{est}}} \quad (7)$$

where R_{th} is the theoretical range of alpha particle energy incident on the detector material.

Track profile was obtained as mentioned before and the range of certain particle track energy in the detector was measured using the relation

$$R = L_{\text{eR}} + h_R \quad (8)$$

where L_{eR} is the track length just very close to the end of track $L_{\text{eR}} = V_T t_R$, V_T is the track etch rate and h is the removal thickness layer ($h = V_B t_R$), t_R is the time needed to reach to the end of track.

3.2.1 The results and discussion of TPT

Table 1 show that the L_{\max} depends on the energy of the incident particle while the t_R not depends only on the energy of the incident particle but also on the etching rates, particularly the bulk etch rate V_B which in turn controlled by the etching conditions; the concentration, and the temperature of the etching solution. The bulk etch rate V_B was varying from 1.21 to 1.28 $\mu\text{m h}^{-1}$ with average value $1.25 \pm 0.04 \mu\text{m h}^{-1}$. All values of V_B were dependent on the etching conditions. The value of L_{\max} for the same energy is constant in the same matter. The range of the particle energy dependent on the density of medium. $R = \int_0^R dx = \int_T^0 \frac{dx}{dT} dT = \int_0^T \frac{dT}{S(T)}$ and $S(T) = -\frac{dx}{dT} dT = \bar{I}n_{\text{ion}}$ where T is the kinetic energy of the particle, n_{ion} is the number of electron ion pairs formed per unit path length, and \bar{I} denotes the average energy needed to ionize an atom in the medium. The concentration of the solution and temperature are used to elucidate the path of the particles and have no effect along the path. The value of L_{\max} does not affect by increase in the concentration or in the temperature of the etching solution, while the time needed to reach to the end of track (t_R) is change with change the condition of etching. The values of L_{\max} were 20.02, 17.60 and 12.32 μm with the energies of alpha particle 5.48, 5 and 4 MeV respectively. The result show that, the range of alpha energies 4, 5 and 5.48 MeV in CR39 were 19.88, 29.89 and 33.88 μm respectively. This value corresponds to the theoretical values shown in **Table 1**. After these regions, the track length starts to turn gradually into a circular path, and the track etch rate approaches the bulk etch rate ($V_T \approx V_B$) and the track begins to change gradually to the spherical shape (**Figure 5**).

3.3 The concentration of radon and the annual effective dose

The equilibrium concentration of radon C_{eq} determined from the track density by using the following relation

$$C_{\text{eq}} = \frac{\rho}{Kt_{\text{ef}}} \quad (9)$$

where t_{ef} is the effective exposure time in hours and the calibration factor K of the SSNTDs ($\text{tracks cm}^{-2} \text{ day}^{-1}/\text{Bq m}^{-3}$).

The surface exhalation rate ($\text{Bq m}^{-1} \cdot \text{h}^{-1}$) of the sample for the release of radon can be calculated by the formula exhalation rate [5, 7].

$$E_a = \frac{C_{\text{eq}}V\lambda}{A} \quad (10)$$

Energy	$E = 5.48 \text{ MeV}$	$E = 5 \text{ MeV}$	$E = 4 \text{ MeV}$
L_{\max} (μm)	20.02	17.60	12.32
R (μm) (theoretical values)	34.20	29.40	19.80
R (μm) experiment	33.88	29.89	19.88
t_R (h)	11.00	9.75	6.00
V_B (by L_{\max})	1.28	1.21	1.25
Average V_B	$1.25 \pm 0.04 \mu\text{m h}^{-1}$		

Table 1.

The maximum track length, range, the saturation time and bulk etch rate with different energy of alpha particle in CR39 detector.

Where A is the cross section area of cup (m^2), V is the effective volume of the cup in m^3 , and λ the decay constant for radon in h^{-1} .

The mass exhalation rate ($Bq\ kg^{-1} \cdot h^{-1}$) in the samples is calculated using the following formula [4, 5, 8]:

$$E_m = \frac{C_{eq} V \lambda}{M} \quad (11)$$

Where M is the mass of sample (kg).

The annual effective dose H ($\mu Sv\ year^{-1}$) was calculated from the following relation.

$$H = C \times D \times F \times T = 25.2 C\ (\mu Sv\ year^{-1}) \quad (12)$$

where, C in $Bq\ m^{-3}$ is the measured mean radon activity concentration in air, F is the indoor equilibrium factor between radon and its progeny (0.4), T is time ($7000\ h\ year^{-1}$) and D is the dose conversion factor $9\ nSv\ h^{-1}/Bq\ m^{-3}$ [3, 9].

3.4 Neutron activation analysis

Thermal neutron activation analysis is used as the primary method for determining the element in any sample. This analysis is carried out inside the reactor with a flow of $3.31 \times 10^{12}\ n\ cm^{-2}$ or more. Long-lived radio nuclides are determined using activation with thermal neutrons. First, the samples are filled in aluminum cups. With a 2-hour irradiation time, then re-encapsulate after irradiation and then measured after 4 days of cooling and a second time after 20 days of cooling, using a high-purity Germanium Mono-Germanium Spectrometer (HPGe) ray with a precision of 2.5 kV for the ^{60}Co 1332.5 keV line, efficiently It is about 40% relative to the 3×3 "NaI reagent of the same line. Then gamma spectra are analyzed and then the concentrations of different detected elements are estimated [10].

This method give the different element in air or in soil for example in Jazan region we can measure the different heavy element in air by using this technique.

3.4.1 The results and discussion of NAA

The Figures 6–9 are summarized the concentrations of heavy elements in Airport and Cady mall in PM_{10} and TSP samples which collected from Jazan city.

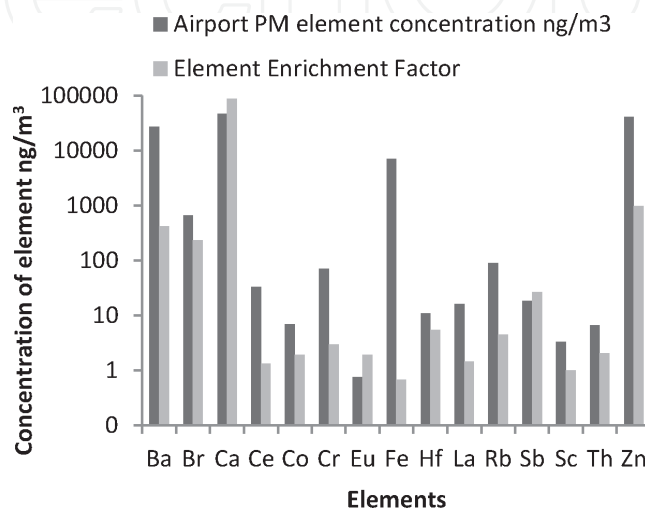


Figure 6.
 PM_{10} —Airport zone: concentrations of heavy elements.

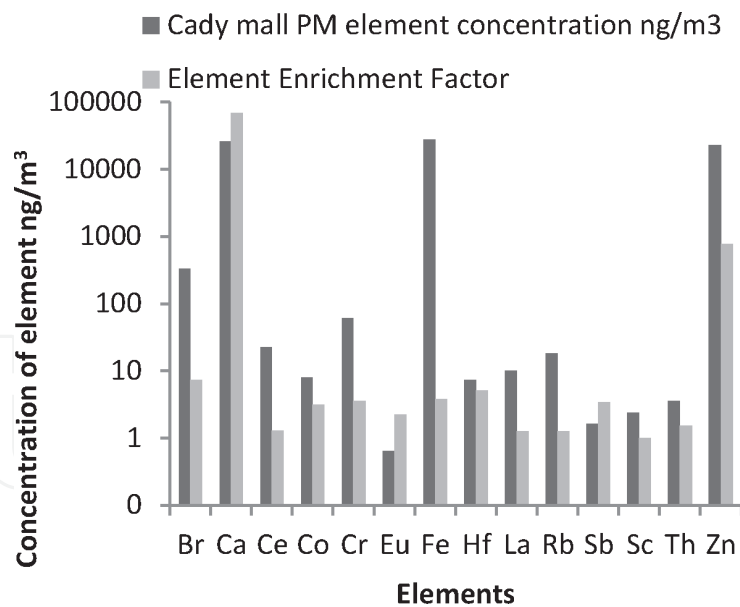


Figure 7.
PM10—Cady mall zone: concentrations of heavy elements.

Figures 6 and 7 were shown that the concentrations of heavy elements in Airport and Cady mall in PM10. The elements in TSP sample show in Figures 8 and 9.

By adopting the level of concentration of elements in the atmosphere as the ranking standard, barium, calcium, iron and zinc elements were found to be the most dominant elements in the Jazan region of Saudi Arabia. It was observed that the concentration depends on the study areas, as the industrial regions had the highest concentration of barium, iron, and zinc, whereas the market areas had the lowest concentration, especially barium and calcium. Barium concluded that the main source of barium traces is car paints. It was also found that the concentration of zinc traces in the airport area and in the industrial zone samples. The main sources of zinc impacts in Jizan are tire wear, brake wear and exhaust emissions. Therefore, we can ensure that zinc emissions are due to industrial processes, especially those related with tire wear and wear. Tires and brake pads are made of

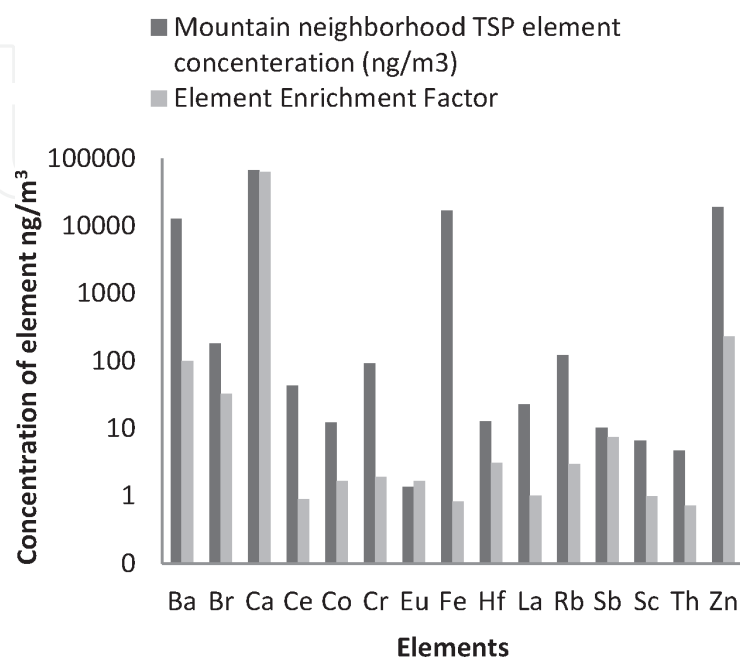


Figure 8.
TSP—Mountain neighborhood zone: concentrations of heavy elements.

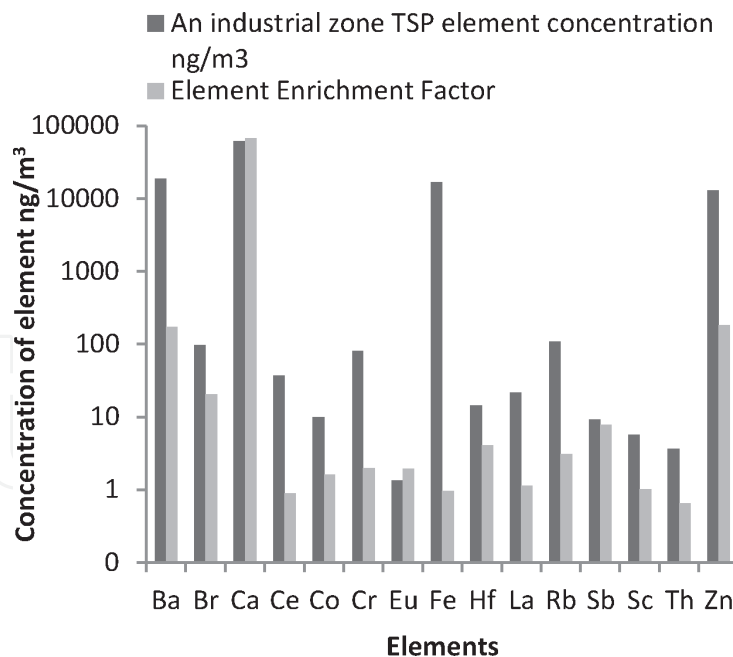


Figure 9.
 TSP—an industrial zone: concentrations of heavy elements.

vulcanized rubber in the presence of a stimulant. The vulcanization tonic currently used in industry is zinc oxide, which explains the source of zinc in tires and brake pads.

The lowest concentrated elements were bromine and chromium in the Jizan region. The effects of bromine can be attributed to vehicle emissions. The contribution of cars to bromine emissions cannot be more than 5%. Chromium TSP concentration was also found from the Jazan mountainous district. Concentration may be harmful based on the findings of the Environmental Protection Agency [11], that continuous inhalation of about 0.8 ng m^{-3} of chromium increases the risk of cancer by $1.0 \times 10^{-6}\%$.

Basically, earth elements include Ce, Eu and La, while trace elements include Sc, Th, Hf, Sb and Co. The maximum concentration of Sc and Co was noted in the Mountain neighborhood samples, while Th and Sb concentrations were found to be highest in the Airport zone. The maximum concentration of Hf was noted in the industrial zone samples, while the highest concentration of La, Ce and Eu was noted in mountain neighborhood samples.

These concentrations differ from site to site according to the geography of the place and the data provided indicate that the concentration of iron, calcium, chromium and zinc in Jazan is relatively less than in other regions. The **Table 2** shows these differences.

3.5 Measurement of gamma ray

To reduce the gamma ray background the hyper pure germanium detector is inserted inside a lead shield, through a hole in the bottom. The lead shield is internally lined with cadmium and copper layers. A layer of Cd ($z = 48$) and Cu are used, Cd is an effective filter for Pb-X rays, while Cu attenuates the Cd-X ray and prevents personal exposure to the toxic cadmium **Figure 10**.

To reduce the noise from the thermal radiation in the crystal, the HPGe detector is cooled with liquid nitrogen (77°K , -194°C) during its use. This reduces the leakage current generated by mobile carriers at room temperature and prevents voltage break down through the crystal. The HPGe Gamma-ray spectrometer

Local	Concentration (ng m ⁻³)					References
	Ca	Fe	Zn	Cr	Co	
Jazan city	26058.8–66998.4	7003.8–27798.7	12955.1–41069.7	61.14–91.9	6.9–12.1	Present work
North Egypt	Nd	1430–22,230	50–146,930	10–500	1–20	EL-Araby et al. [10]
Upper-Egypt	42713.43–80447.75	2022.23–21,420	12327.1–25628.3	59.9–101.55	7.3–12.24	Monged [12]
Santa Cruz, Brazil	11–2.5 × 10 ⁵	77.4–2.9 × 10 ⁵	0.0–1.5 × 10 ⁴	0.0–8678	0.8–1.6	Quiterio et al. [13]
La Plata, Argentina	Nd	747–5967	20–1049	3.5–12	Nd	Bilos et al. [14]
Birmingham, UK	171–245	245–348	64–641	7.1–18	Nd	Harrison et al. [15]
East St. Louis, USA	1918	666	231	5.7	Nd	Sweet et al. [16]
USA and European Cities	Nd	3710	<10 ³	10–30	Nd	Lantzy and Mackenzie [17]

Table 2.

Comparison of the concentration ranges of some elements in Jazan (present work) and other places in the world.

consists of a detector, a pulse processing electronic unit, and an output device such as a counter, multi-channel analyzer (MCA). A diagram of a basic radiation detection system is **Figure 11**.

The coarse and fine gain controls of the spectroscopy amplifier, its differentiating and integrating time constants and all other controls were adjusted to obtain the best energy resolution and good linearity of the spectrometer over a wide range the input voltages. After selecting the optimum set up, the resolving power (resolution) of the spectrometer was found to be 1.92 KeV for 1332 KeV gamma ray line of the ⁶⁰Co.

The gamma ray spectrometer system was calibrated by applying different standard gamma emitters' sources. These include ¹³⁷Cs (661.66 keV), ⁶⁰Co (1173.23, 1332.5 keV), ⁴⁰K (1460.8 keV) and ²²⁶Ra which is most favorable for calibration, since its spectrum covers a wide energy range from 0.186 to 2.45 MeV.

To measure gamma ray in any sample must folded and placed container for 1 month to allow radioactive equilibrium to be reached (secular equilibrium) This step ensured that radon gas and its daughters remain in the sample.

The gamma ray spectra of sample accumulate for at least 24 hours, and then analyze to detect the gamma ray energies due to uranium, thorium and their daughters, and due to potassium, and then the counting rate for each gamma transition was determined.

The radioactive decay series of ²³⁸U and ²³²Th are complex and produces alpha, beta, and gamma radiation. **Figures 12** and **13** show the important isotopes in the decay series, indicates whether the primary decay mode is via alpha or beta emission, and gives the half-life.

3.6 Conclusions

This chapter presented the methods of decay for alpha, beta, and gamma, as well as showed the best methods for measuring both alpha and gamma, which are

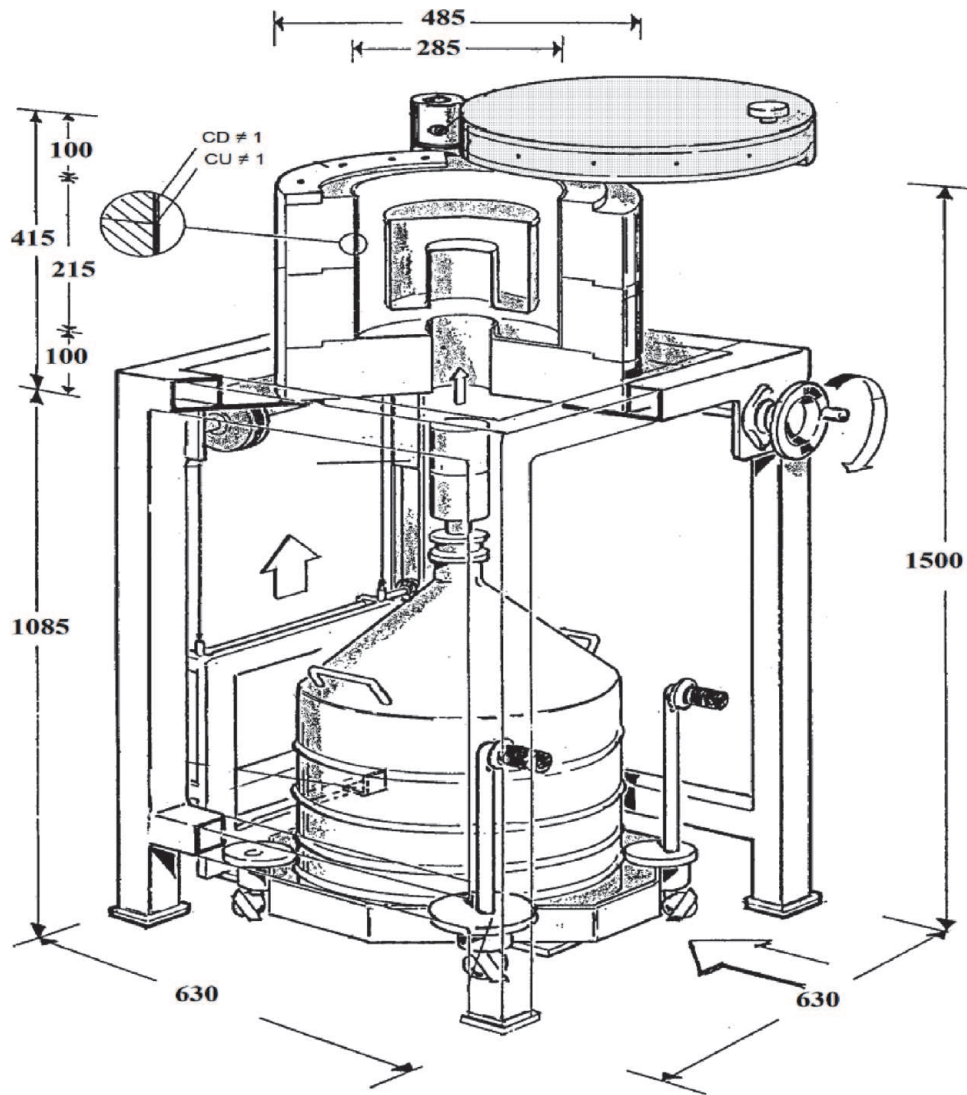


Figure 10.
High purity germanium detector.

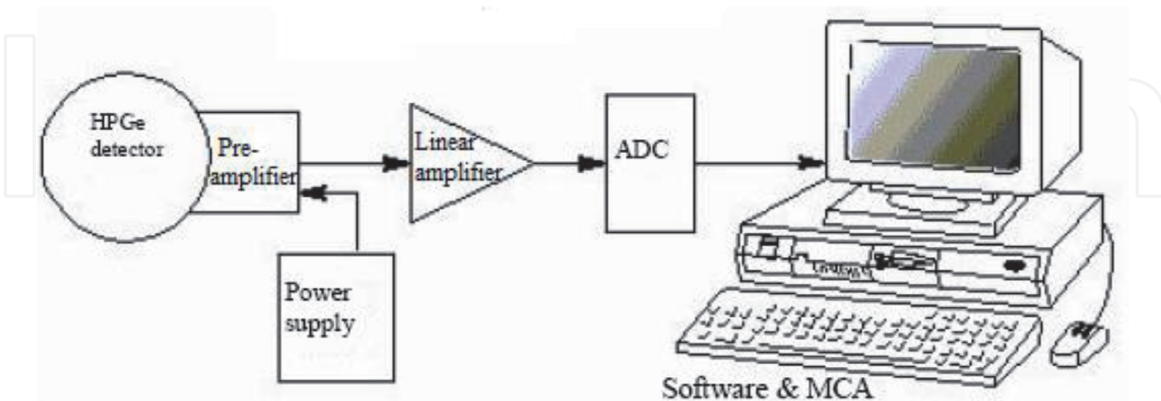


Figure 11.
Block diagram of gamma ray spectrometer.

available and simple, as they are characterized by accuracy and high sensitivity, so it can be relied upon to determine the concentration of radioactive materials and doses that determine the places of pollution. These methods contribute to preserving the environment, by identifying the places of pollution, whether by radiation or by heavy materials. Measuring heavy materials is an important technology in

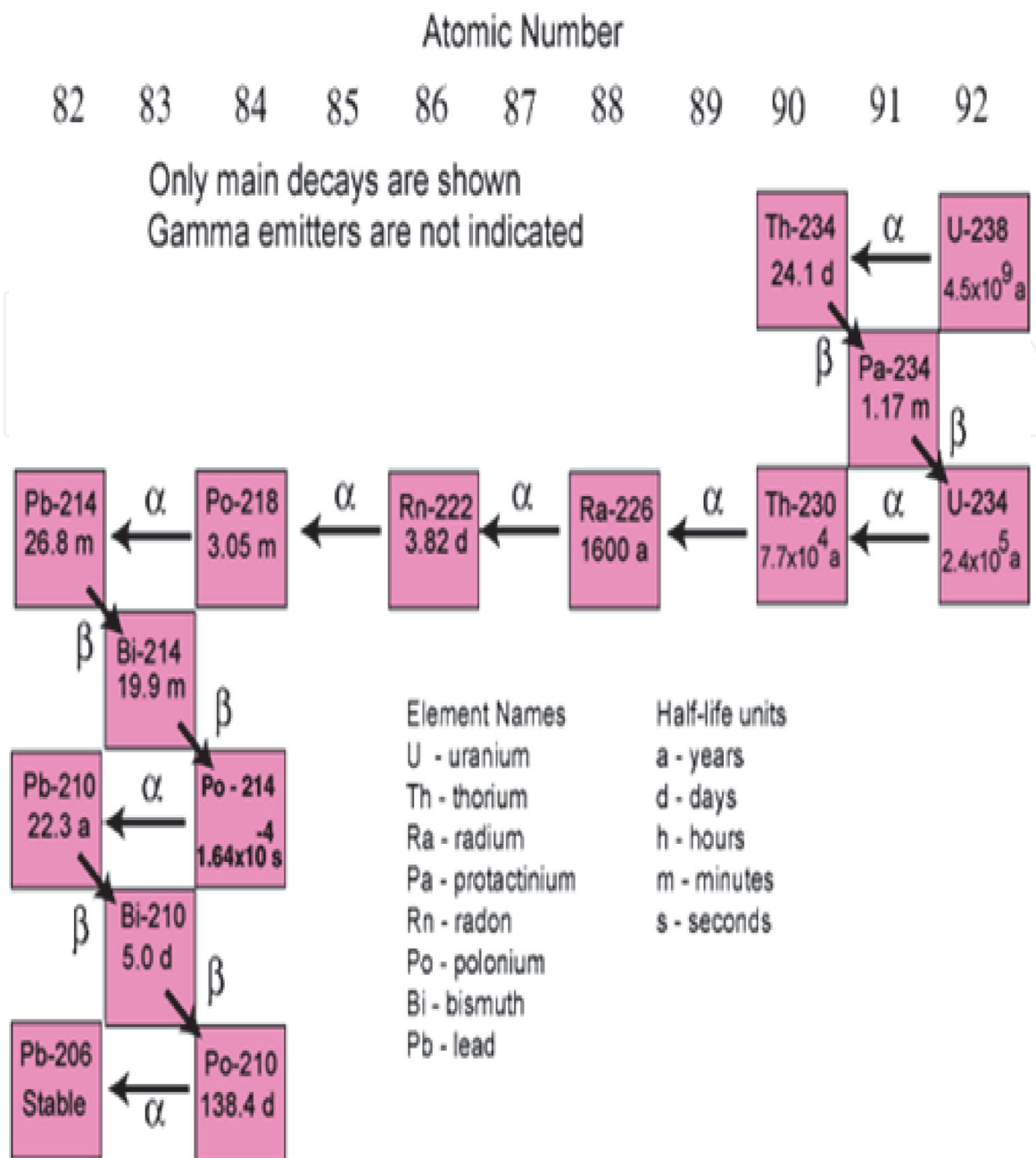


Figure 12.
The Uranium-238 decay chain.

determining the whereabouts of uranium and its daughter. This technology also contributes to reducing environmental pollution by harmful heavy materials.

The result show that the best method to determination of bulk etch rate V_B is by L_{max} method; it is the faster and easier than weight method. The range of alpha particle is measured by track profile method (TPT). The measured range of alpha particles was very close to the theoretical values of the range. The track profile method is useful to determine the different parameters of track.

This chapter has successfully evaluated the concentration of heavy metals in the atmosphere of the Mountain Neighborhood, Airport, Cady Mall and Industrial zones and established a number of conclusions. For instance, it was found that all the sampled specimens were enriched with both zinc and calcium. However, barium was only found in the Airport, Mountain Neighborhood and Industrial zones. Ultimately, a number of conclusions based on the findings have been outlined below.

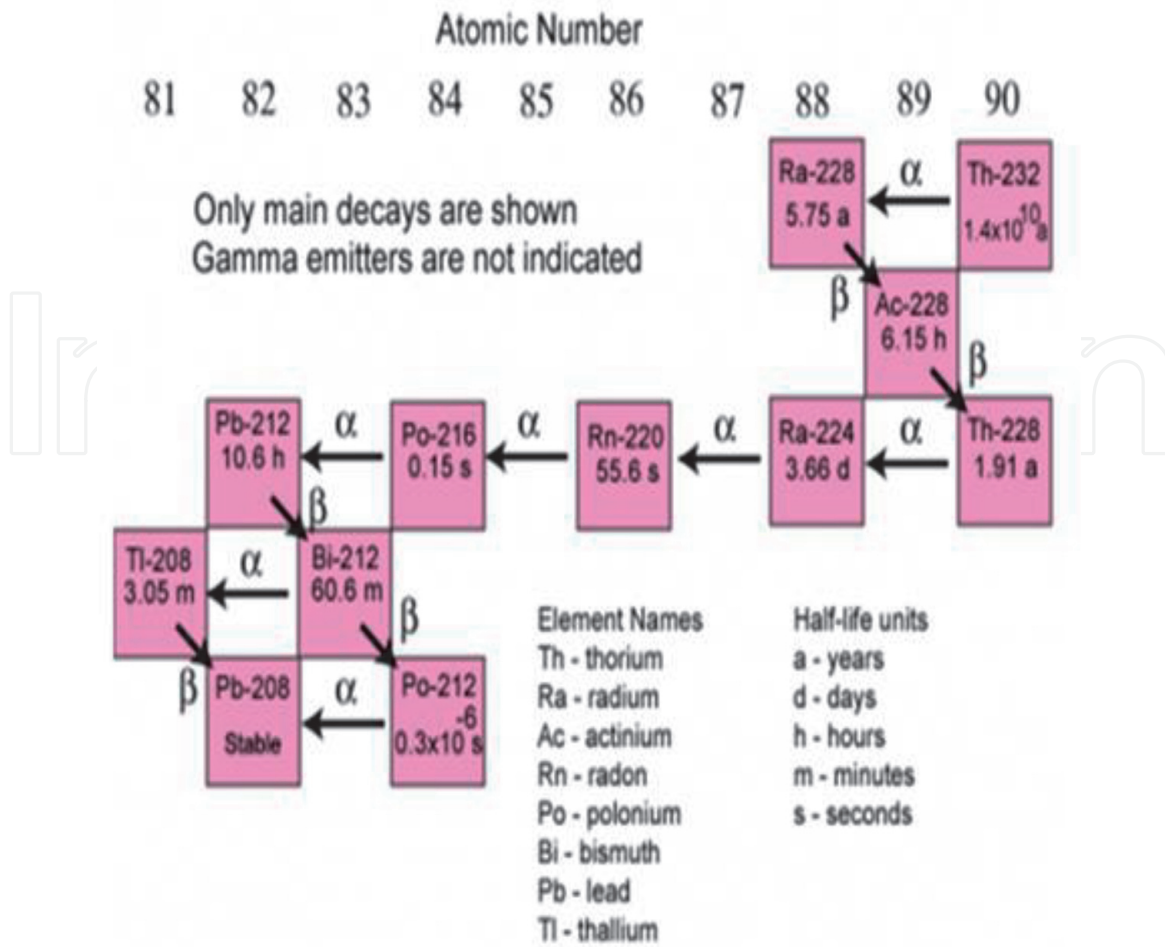


Figure 13.
 The Thorium-232 decay chain.

- The analysis of the samples enabled the author to arrive at the conclusion that maximum concentration of PM10 and TSP aerosols in Jazan city occurs during March.
- When literature values for the concentration of heavy metals were compared with other areas, it was concluded that Jazan city had relatively lower concentration with respect to North Egypt and Santa Cruz industrial district. The results also revealed that the difference in heavy metal concentrations was much pronounced when non-polluted zones were compared with polluted zones.
- It was concluded that Jazan city PM10 and TSP aerosols are mainly rich in calcium, barium, zinc, and iron; all of which are as a result of anthropogenic activities.
- The concentration of zinc and Barium was found to be highest in the airport area, while iron and calcium were found to be highly concentrated in Cady Mall and the Mountain neighborhood respectively.

Having covered the concentration of heavy metals in the atmosphere of four locations in Jazan city, and the dangers associated with high concentration of such metals ascertained, a number of recommendations were made as follows.

It is recommended that green belts be designed around different cities in order to reduce the level of concentration of aerosols in the atmosphere. In addition, environmental regulations should be put forward and their effectiveness be ensured through strict monitoring of air pollution levels. The use of transport and construction machinery that increase emission of aerosols should be minimized whenever possible. Finally the author suggests that a thorough evaluation should be carried out before any industrial project is implemented in order to ascertain its level of pollution as well as its compatibility within the framework of sustainable environment.

IntechOpen

IntechOpen

Author details

Entesar H. Elaraby
Faculty of Science, Jazan University, Kingdom of Saudi Arabia

*Address all correspondence to: entesar.araby@gmail.com

IntechOpen

© 2020 The Author(s). Licensee IntechOpen. This chapter is distributed under the terms of the Creative Commons Attribution License (<http://creativecommons.org/licenses/by/3.0>), which permits unrestricted use, distribution, and reproduction in any medium, provided the original work is properly cited. 

References

- [1] Morison I. Introduction to Astronomy and Cosmology. Southern Gate, Chichester, West Sussex, United Kingdom: John Wiley & Sons Ltd; 2008
- [2] WHO, Handbook. World Handbook on Indoor Radon. World Health Organization. 2009:94
- [3] ICRP. Radiological protection in medicine. ICRP Publication 105. Annals of the ICRP. 2007;**37**(5)
- [4] EL-Araby EH. Direct measurement of the radioactive radon gas activity in water in Saudi Arabia. AIP Conference Proceedings. 2018;**1976**(1):020019
- [5] EL-Araby EH, Soliman HA, Abo-Elmagd M. Measurement of radon levels in water and the associated health hazards in Jazan—Saudi Arabia. Journal of Radiation Research and Applied Science. 2019;**12**(1):31-36
- [6] Azooz AA, AL-Nia'emi SHS, Al-Jubbori MA. Empirical parameterization of CR-39 longitudinal track depth. Radiation Measurements. 2012;**47**:67-72
- [7] Chen J, Whyte J, Ford K. An overview of radon research in Canada. Radiation Protection Dosimetry. 2015; **167**:44-48
- [8] Singh K, Sengupta D, Prasad R. Radon exhalation rate and uranium estimation in rock samples from Bihar uranium and copper mines using the SSNTD technique. Applied Radiation and Isotopes. 1999;**51**:107-113
- [9] UNSCEAR. United Nations Scientific Committee on the Effects of Atomic Radiation Sources and Effects of Ionizing Radiation. United Nations Publication Annex B; 2008
- [10] EL-Araby EH, Abd El-wahab MM, EL-Desouky TM, Diab HM, Mohseen MM. Assessment of atmospheric heavy metal deposition in Egypt by using neutron activation analysis. Applied Radiation and Isotopes. 2011;**69**:1506-1511
- [11] Environmental Protection Agency EPA. Air Toxics Website. 2003. Available from: <http://www.epa.gov/ttn/atw/hlthef/S>
- [12] Monged MHE. Assessment of Ambient Gamma Radiation and Chemical Pollutants in Upper Egypt's Atmosphere. [PhD thesis] Chemistry Department, Faculty of Science, Ain Shams University. 2009
- [13] Quiterioa SL, da Silvaa CRS, Arbilla G, Escaleira V. Metals in airborne particulate matter in the industrial district of Santa Cruz, Rio de Janeiro, in an annual period. AE International-Central & South America, Atmospheric Environment. 2004;**38**: 321-331
- [14] Bilos C, Colombo JC, Skorupka CN, Rodrigues Presa J. Sources, distribution and variability of airborne trace metals in La Plata City area, Argentina. Environmental Pollution. 2001;**111**: 149-158
- [15] Harrinson RM, Smith DJT, Luhana L. Source apportionment of atmospheric polycyclic aromatic hydrocarbons collected from an urban location in Birmingham, UK. Environmental Science and Technology. 1996;**30**:825-832
- [16] Sweet CW, Vermette SJ, Landsberg S. Sources of toxic trace elements in in urban air in Illinois. Environmental Science and Technology. 1993;**27**(12):2502-2510
- [17] Lantzy RJ, Mackenzie FT. Atmospheric trace metals: Global cycles and assessment of man's impact. Geochimica Cosmochimica Acta. 1979;**43**: 511-525